



Faculty of Women for, Arts,  
Science, and Education



Scientific Publishing Unit



# Journal of Scientific Research in Science

Basic Sciences

Volume 40, Issue 1, 2023

ISSN 2356-8372 (Online) \ ISSN 2356-8364 (print)





Contents lists available at EKB

Journal of Scientific Research in Science

Journal homepage: <https://jsrs.journals.ekb.eg/>

## Laser Raman micro spectroscopy and high frequency dielectric properties of silica- xerogel loaded with different concentrations of $\alpha$ -Fe<sub>2</sub>O<sub>3</sub>

Reham Kamal Abd El Hamid<sup>1\*</sup> and Naglaa Ahmed Shahin<sup>1</sup>

<sup>1</sup>Faculty of Women for Arts, Science and Education, Ain-Shams University, Cairo, Egypt.

### Abstract

Sol-gel derived nano-composites silica-gel doped with different iron oxide concentrations at (3.5, 11, 33 and 37 mol. %) sintered at constant temperature at 1170°C, are illustrated in this work. Structure, surface morphology, high frequency dielectric and magnetic trends of the mentioned nano-composites analyzed and investigated through XRD, UV-Vis, TEM, FESEM and Magnetic hysteresis curves. Raman micro-spectroscopy gives rise to samples homogenous distribution. XRD illustrate that the Hematite ( $\alpha$ -Fe<sub>2</sub>O<sub>3</sub>) is the optimum phase rather than the Maghemite ( $\gamma$ -Fe<sub>2</sub>O<sub>3</sub>) and Magnetite ( $\epsilon$ -Fe<sub>2</sub>O<sub>3</sub>). Big amount of Hematite ( $\alpha$ -Fe<sub>2</sub>O<sub>3</sub>) crystalline nano-particles are expected at 37 mol. % of Fe<sub>2</sub>O<sub>3</sub>. XRD confirmed that the average crystallite size increased from (25-31) nm with increasing the concentration of ( $\alpha$ -Fe<sub>2</sub>O<sub>3</sub>) from 3.5 up to 37 mol%. The A.C. conductivity  $\sigma_{ac}$  increased by increasing the  $\alpha$ -Fe<sub>2</sub>O<sub>3</sub> content, according to the presence of oxygen vacancy and the crystalline size increases. The decreasing behavior in magnetization value ( $M_s$ ) is related to the changes of the crystallite size, magnetic iron oxide particles and concentration. All analysis explains Hematite is extremely stable at ambient conditions and at high temperatures, so it is the better for particular applications.

**Keywords:** iron oxide; sol gel; laser Raman micro spectroscopy; Impedance analyzer (KEYSIGHT-E4991B).

### 1. Introduction

In modern research, transition metal oxide nanoparticles attracted a large attention because of their electrical and optical properties making them suitable for application in different kinds of opto-electronic devices<sup>[1]</sup>, also have been at the heart of many dramatic advances in the material science<sup>[2]</sup>, for these potential technological applications. Iron oxide has different phases, namely hematite ( $\alpha$ -Fe<sub>2</sub>O<sub>3</sub>) anti ferromagnetic, maghemite ( $\gamma$ -Fe<sub>2</sub>O<sub>3</sub>) ferromagnetic and magnetite ( $\epsilon$ -Fe<sub>2</sub>O<sub>3</sub>). Hematite ( $\alpha$ -Fe<sub>2</sub>O<sub>3</sub>) is the most stable iron oxide under ambient conditions. It is a low cost non-toxic environment friendly material easily available in nature<sup>[3]</sup>.  $\alpha$ -Fe<sub>2</sub>O<sub>3</sub> shows antiferromagnetic (weakly ferromagnetic) at room temperature shows

\*Corresponding author: Reham Kamal Abd El Hamid, Physics Department, Faculty of Women for Arts, Science and Education, Ain Shams University, Egypt.

E-mail: [reham.kamal@women.asu.edu.eg](mailto:reham.kamal@women.asu.edu.eg)

(Received 18 December 2022, revised 09 February 2023, accepted 16 February 2023)

<https://doi.org/10.21608/JSRS.2023.181572.1098>

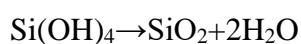
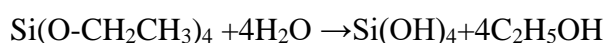
paramagnetic above temperature of 948K<sup>[4]</sup>.  $\alpha$ -Fe<sub>2</sub>O<sub>3</sub> displays wide ranges of applications such as, catalysis<sup>[5]</sup>, gas sensors<sup>[6]</sup>, solar cells<sup>[7]</sup>, magnetic resonance imaging<sup>[8]</sup>, pigments<sup>[9]</sup>, and spin electronic devices<sup>[10]</sup>. Silica nanoparticles have gained importance in recent years because of their applications in various areas and easy synthesis process. Surface modification opens up the door for its future application in the field of biotechnology and medicine such as for cancer treatment, dental filling composites and drug delivery<sup>[11]</sup>. The silica gels are suitable for this application due to their high porosity, inertness chemical, large accessible surface area and transparency<sup>[12]</sup>, also Silica have also been used as cell markers, catalytic substrates, absorbents, and matrix fillers<sup>[13]</sup>. Fe<sub>2</sub>O<sub>3</sub>/SiO<sub>2</sub>, nano-composites have interesting properties and applications in catalysis, sensing and magnetism<sup>[14-15]</sup>. The conventional materials change their thermal, optical, magnetic properties in nano form corresponding to surface area increased and quantum effect. Recently, the magnetic nano particles (ferrite nano materials) have much attention and show interesting properties in many fields such as data storage, optical fiber, biomedical and medical fields etc....Sol gel is mainly interesting method due to its low cost, high purity, short preparation time, and homogenous solution of doping element and magnify the excellent polycrystalline samples. Information about A.C. conductivity can be gained by studying the influences of frequency and temperature on dielectric properties of different nano-composites<sup>[16]</sup>. The silica xerogel beads embedded with Fe<sub>2</sub>O<sub>3</sub> nanoparticles used for more column stability to remove the product gases from the reactants without clogging the column unlike in the powder samples<sup>[17]</sup>. The Fe<sub>2</sub>O<sub>3</sub> nanoparticles immobilized on SiO<sub>2</sub> support is explored, anticipating that the Fe<sub>2</sub>O<sub>3</sub> - SiO<sub>2</sub> interactions may prevent self-agglomeration of Fe<sub>2</sub>O<sub>3</sub> nanoparticles<sup>[18]</sup>

The properties of Fe<sub>2</sub>O<sub>3</sub>/SiO<sub>2</sub> materials in fact, depend on the nature of the interaction between silica xero-gel and iron oxide. Increasing temperature and/or iron concentrations the prepared samples are assumed to cause changes in the bond lengths and/or bond angles of the structural silicate units within network. In this work, Silica doped with Iron-oxide in different molar ratios 3.5, 11, 33 and 37 mol.%, were synthesized with the sol gel process sintered at 1170°C. The prepared nano-composite materials were characterized with laser Raman micro spectroscopy, X-Ray Diffract meter (XRD). The prepared samples compatibility was investigated by SEM. The dielectric parameters of the samples were studied for first time in a wide range of frequencies (1 MHz - 1 GHz). Finally, many efforts will be done to find the possibility to use the studied nano-composite prepared samples as promising candidates for sensors and magnetic devices.

## 2. Experimental

A composite of silica gel and different concentration of iron oxide was prepared by modified sol-gel process. By mixing tetra-ethoxy-silane,  $(\text{CH}_3\text{CH}_2\text{O})_4\text{Si}$  (TEOS) (Aldrich, 98%), ethyl alcohol ( $\text{CH}_3\text{CH}_2\text{OH}$ ), distilled water and HCL with molar ratios 0.28: 0.174: 0.028: 0.0823 respectively.<sup>[19]</sup>

An aqueous solution of iron nitrate ( $\text{Fe}(\text{NO}_3)_3 \cdot 9\text{H}_2\text{O}$ ) was introduced in the initial stage of the process with different concentrations (3.5, 11, 33 and 37 mol %) to dope the silica giving nano-composites. These solutions were stirred for one hour. The clear sol was then poured into a Teflon beaker and allowed to gel in air. The gel was dried in an oven for one week by slowly raising the temperature up to  $100^\circ\text{C}$  <sup>[20]</sup>, and then kept for 24 h at  $150^\circ\text{C}$ . Heating steps between  $50^\circ\text{C}$  and  $1170^\circ\text{C}$  at each temperature for 30 min respectively. After the treatment at higher temperature the samples changed and looked like ceramics. The overall process can be written as:



## 3. Characterization techniques:

The X-ray diffraction (XRD) patterns for the prepared samples are recorded with a Philips X-ray diffractometer using mono-chromatized  $\text{CuK}_\alpha$  radiation of wavelength  $1.54056\text{\AA}$  from a fixed source operated at 45 kV and 9 mA. Absorption spectra (200-1800 nm) were measured using a The Model V-570 UV/VIS/NIR spectrophotometer. The instrument specified by resolution 0.1 nm and wavelength accuracy  $\pm 0.3$  nm (at a spectral bandwidth of 0.5 nm). The Raman single point measurement using Alpha 300 RA/S from Witec-Ulm Germany is used with 532 nm laser and 100X Zeiss objective. The morphology of the prepared samples was depicted by using high resolution field emission gun quanta FEG 250 scanning electron microscope (FE-SEM). The FE-SEM gives information on the samples surface morphology. Dielectric properties were measured in a wide range of frequencies between 1 MHz and 1 GHz using network impedance analyzer (KEYSIGHT-E4991B).

## 4. Results and discussion

### X-Ray diffraction (XRD) characterization:

The composition and crystalline phase purity of silica gel doped with different iron oxide concentration at (3.5, 11, 33, and 37 mol %) sintered at  $1170^\circ\text{C}$  were examined by XRD

pattern in the  $2\theta$  range of 10-80 degrees are shown in Figure (1:a→d). In all the cases a hump due to amorphous silica phase is visible at  $2\theta \sim 22$  degrees (mineral name: cristobalite, tetragonal crystal system, ICSD card No. 47219) [21]. Also It is clearly seen that many diffraction peaks detected at  $2\theta = 22^\circ, 26^\circ, 28.4^\circ, 31.9^\circ, \text{ and } 36.5^\circ$  corresponding to  $\alpha\text{-Fe}_2\text{O}_3$  (mineral name: Hematite, Rombohedral phase, JCPDS card No. (98-017-3024)) indexed as (111),(120),(121),(031) and (201) respectively. Moreover, the figure illustrates some distinct characteristic peaks at  $23.8^\circ, 32.8^\circ, 35.2^\circ, 40.2^\circ, 49.1^\circ, 53^\circ$  and  $62.5^\circ$ , which are ascribed to  $\alpha\text{-Fe}_2\text{O}_3$  with preferred orientations (012),(122),(200),(132),(142),(204) and (026). Also, other very weak peaks are observed at  $57.9^\circ, 63.3^\circ, 71.7^\circ$  and  $75.3^\circ$  attributed to  $\gamma\text{-Fe}_2\text{O}_3$  (mineral name maghemite, spinel structure with disordered vacancies, cubic crystal system)[22-23] and  $\epsilon\text{-Fe}_2\text{O}_3$  with preferred orientations as(035), (330),(235) and (401), respectively.[24] By increasing the  $\text{Fe}_2\text{O}_3$  content on the host silica gel, it has been reported that the peaks intensity increased and shifted to higher  $2\theta^\circ$  at 37 mol % of  $\text{Fe}_2\text{O}_3$  suggesting a growing of crystal domain size[25]. Moreover, it can be noticed that the principal tetragonal  $\alpha$ - cristobalite peak is observed at  $2\theta^\circ = 22^\circ$  index at (111) increased and changed by increasing the  $\text{Fe}_2\text{O}_3$  concentration due to the rearrangement acting in the structure as a result of doping with iron oxide. The obtained data revealed that the hematite  $\alpha\text{-Fe}_2\text{O}_3$  is the major phase and a very minor component of  $\gamma\text{-Fe}_2\text{O}_3$  and  $\epsilon\text{-Fe}_2\text{O}_3$  in all the samples, pointing to high purity and succession of the nano-composite samples preparation. It has been noticed that the annealing at high temperature  $1170^\circ\text{C}$  and increasing the concentration gives rise to the crystallization into the more stable  $\alpha\text{-Fe}_2\text{O}_3$ . The average crystalline sizes calculated using Scherer's equation [26] from the principle peak were found to be equal to 25,26, 27 and 31 nm for 3.5,11,33 and 37 mol%, respectively. One can conclude that the Hematite ( $\alpha\text{-Fe}_2\text{O}_3$ ) phase is the dominant phase in all samples. [27] Lattice parameters of the synthesized of  $\alpha\text{-Fe}_2\text{O}_3, \epsilon\text{-Fe}_2\text{O}_3$ , and  $\gamma\text{-Fe}_2\text{O}_3$  nanoparticles are tabulated in Table 1.

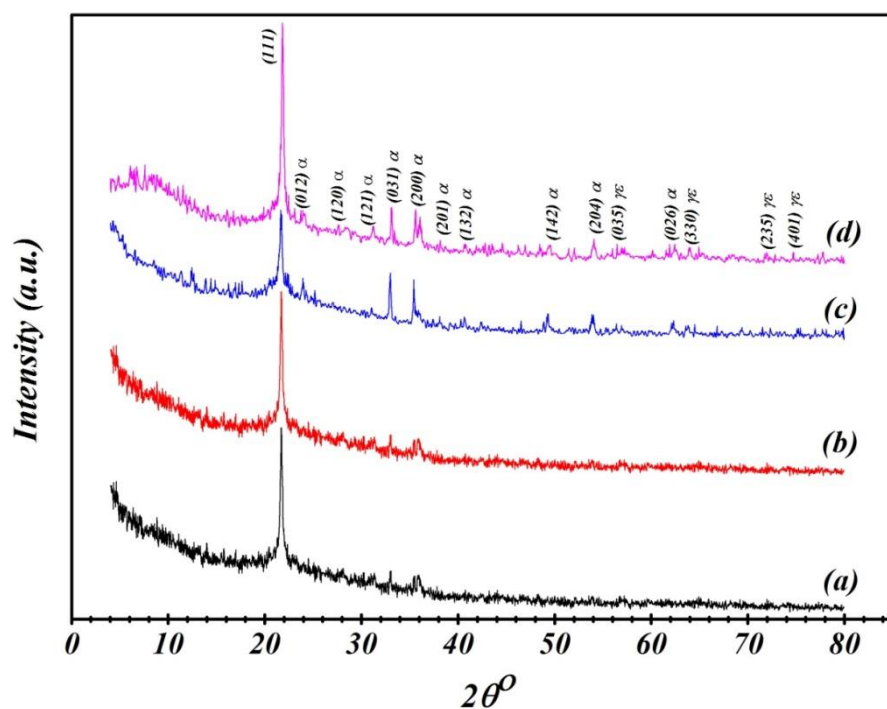


**Figure 1.** The XRD of silica gel doped with different concentration of  $\text{Fe}_2\text{O}_3$  (a) 3.5,(b) 11, (c) 33and(d) 37mol%, respectively sintered at  $1170^\circ\text{C}$ .

**Table.1:** Crystallographic data obtained from XRD of  $\alpha\text{-Fe}_2\text{O}_3$   $\varepsilon\text{-Fe}_2\text{O}_3$ , and  $\gamma\text{-Fe}_2\text{O}_3$

property	Hematite	Magnetite	Maghemite
Molecular formula	$\alpha\text{-Fe}_2\text{O}_3$	$\varepsilon\text{-Fe}_2\text{O}_3$	$\gamma\text{-Fe}_2\text{O}_3$
Crystallographic	Rhombohedral	Cubic	Cubic
Lattice parameter(nm)	a=0.508 ,b=0.878 ,c=0.947	a=0.939 ,b=0.939 ,c=0.939	a= 0.928 ,b=0.928 ,c=0.928
Relative percentage	44.6%	1.4%	1.3%

Applications	Catalysts, pigments, gas sensors				Solar energy conversion, drug delivery, environmental catalysis, recording devices	Magnetic recording, high frequency switch modes, electromagnetic absorbers
Crystalline size of $\alpha$ -Fe <sub>2</sub> O <sub>3</sub>	3.5mol % 25 nm	11mol % 26nm	33mol % 27nm	37mol % 31nm		

### TEM and SEM analysis:

Transmission electron microscopy (TEM) of the  $\alpha$ -Fe<sub>2</sub>O<sub>3</sub> (3.5 mol%)/SiO<sub>2</sub> sample annealed at 1170°C are shown in figure (2). From the figure it is clearly exhibit that the SiO<sub>2</sub> particles are spherical with particle size in range ~ 30-50 nm. The small dots could be noticed, which may be due to  $\alpha$ -Fe<sub>2</sub>O<sub>3</sub> in form of spherical. The crystalline nano particle size of Fe<sub>2</sub>O<sub>3</sub> is ~ 24 nm. This indicates the uniform dispersion of Fe<sub>2</sub>O<sub>3</sub> grains on silica matrix.

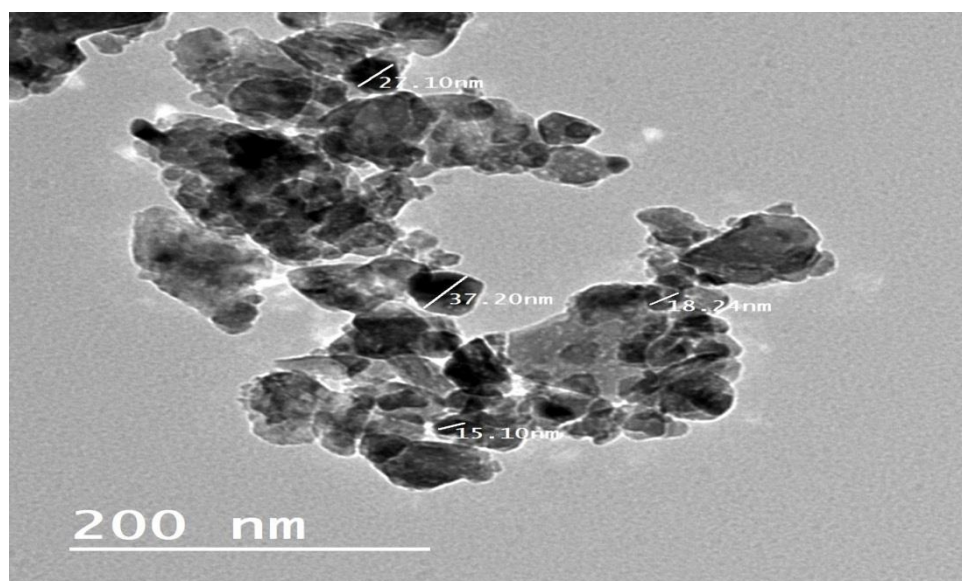


**Figure 2. TEM micrograph of silica gel doped with 3.5 mol% of  $\alpha$ -Fe<sub>2</sub>O<sub>3</sub>, sintered at 1170°C.**

High resolution Surface electron microscopy (FESEM) images of  $\alpha$ -Fe<sub>2</sub>O<sub>3</sub> (37mol%)/SiO<sub>2</sub> nano-composite sintering at 1170°C is shown in figure(3). The mean grain size is in the nano-scale range, even at higher iron concentration calculated by the XRD. The SEM micro-graph shows a uniform grain size distribution, a fine monolith size and homogeneous microstructure appeared as shown in figure.3. In the graph, we can observe large particles were distribution over the bulk gel, which consists diffraction lines appear in the XRD patterns, whose peak positions are assigned to  $\alpha$ -Fe<sub>2</sub>O<sub>3</sub> phase.

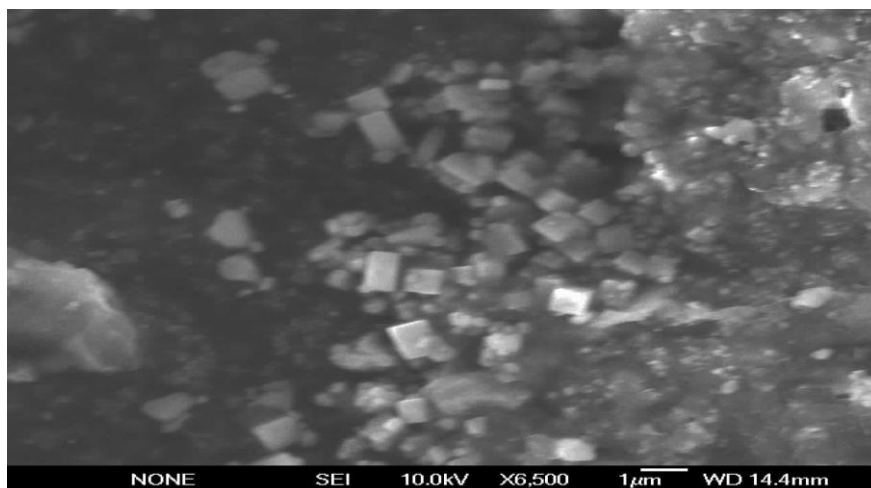


**Figure 3. FESEM image of silica gel doped with 37 mol% of  $\alpha$ -Fe<sub>2</sub>O<sub>3</sub>, sintered at 1170°C.**

#### UV-vis spectroscopy:

To estimate optical properties of the  $\alpha$ -Fe<sub>2</sub>O<sub>3</sub> (3.5→37)mol%/SiO<sub>2</sub> sintered at 1170°C, the UV-vis absorption spectra in wavelength range (200-800)nm are showed in figure(4). The figure illustrated the  $\alpha$ -Fe<sub>2</sub>O<sub>3</sub> have two absorption peaks in wave length ranges of the ultraviolet and visible light, respectively. The first region ranged from 238 to 353nm is assigned to the transfer spectra between metal and silica matrix, and the second region ranged from 500 to 575nm is the finger print region of hematite. Moreover, the absorption strength of the  $\alpha$ -Fe<sub>2</sub>O<sub>3</sub> / SiO<sub>2</sub> increases with the increase of Fe<sub>2</sub>O<sub>3</sub> content. These facts may be attributed to the transition in crystal field and the charge transfer process, which increased with increasing Fe<sub>2</sub>O<sub>3</sub>.<sup>[ 28 ]</sup> Furthermore, the band gap energies of the  $\alpha$ -Fe<sub>2</sub>O<sub>3</sub> / SiO<sub>2</sub> could be estimated by the following equation<sup>[29]</sup>

$$E_g = 1240 / \lambda_g \quad (1)$$

Where  $E_g$  is the band gap energies of the  $\alpha$ -Fe<sub>2</sub>O<sub>3</sub> /SiO<sub>2</sub> nanocomposite,  $\lambda_g$  is the wavelength at the overlap of the vertical and horizontal portions on the band edge.

As seen in figure(4), the values of  $\lambda_g$  is shifted to higher wavelength with increasing  $\alpha$ -Fe<sub>2</sub>O<sub>3</sub> concentration, which shifts from 550 to 575nm corresponding to band gap energy from 2.25 eV to 2.15 eV respectively. This result illustrated that the value of band gap of nanocomposite decreased with increasing  $\alpha$ -Fe<sub>2</sub>O<sub>3</sub> nanoparticle, also the reduction in the band gap is due to increase in the grain size.<sup>[30]</sup>

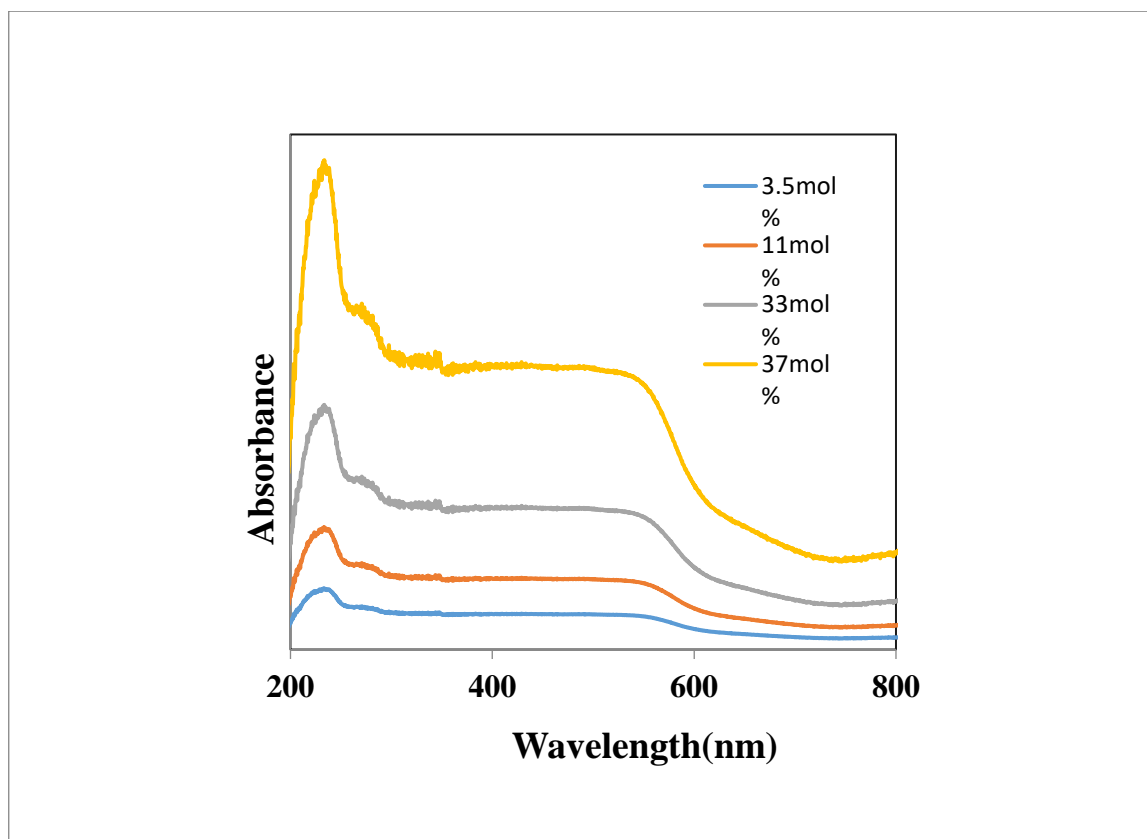


**Figure 4. UV-vis Absorbance of silica gel doped with different concentration of  $\alpha$ -Fe<sub>2</sub>O<sub>3</sub> (3.5→37)mol%/SiO<sub>2</sub>, sintered at 1170°C.**

### Raman spectrum

Raman spectroscopy for silica gel doped with different concentration 3.5, 11 33 and 37mol% of Fe<sub>2</sub>O<sub>3</sub> sintered at 1170°C, is observed in Fig(5), respectively. The most pronounced Raman bands for the prepared samples are given and assigned in Table (1). The low intense peak appeared at about 1070 Cm<sup>-1</sup> is according to Si-O-Si stretching vibrating bond asymmetric. The small peaks at 820 Cm<sup>-1</sup> are attributed to the Si-O-Si symmetric stretching vibrating mode. The Raman spectra at 496 and 609 Cm<sup>-1</sup> corresponding to the presence of Si-O rings for 4 and 3-fold, respectively.

The appearance of the peak at 413 Cm<sup>-1</sup> could be attributed to Si-O-Si, bending oxygen mode. Band with sharp intensity located at 228 Cm<sup>-1</sup> is the fingerprint of the Raman spectrum

of  $\alpha$ -cristobalite. These results are compatible with that obtained from XRD patterns and previous studies. The observed difference is the sharpness of the appeared peaks of samples, which may be due to the increase of the degree of crystallinity as indicated by XRD. Also, from the table (2), shows the assigned bands corresponding to  $\alpha$ -Fe<sub>2</sub>O<sub>3</sub> (hematite) phase [31].

**Table (2): Raman bands assignment of silica gel doped with different concentration of Fe<sub>2</sub>O<sub>3</sub>: 3.5, 11, 33 and 37mol%, respectively sintered at 1170° C**

Raman bands					The assignment
SiO <sub>2</sub> /Fe <sub>2</sub> O <sub>3</sub>	3.5 mol%	11 mol%	33 mol%	37 mol%	
228 Cm <sup>-1</sup>	223	223	223	226	$\alpha$ -cristobalite
-----	292	289	292	294	$\alpha$ -Fe <sub>2</sub> O <sub>3</sub>
430 Cm <sup>-1</sup>	430	430	430	430	Si-O-Si bending oxygen mode
-----	404	407	413	413	$\alpha$ -Fe <sub>2</sub> O <sub>3</sub>
496 Cm <sup>-1</sup>	496	496	496	496	Four and three-fold Si-O rings
609 Cm <sup>-1</sup>	609	609	609	609	Four and three-fold Si-O rings
-----	609	611	619	608	$\alpha$ -Fe <sub>2</sub> O <sub>3</sub>
820 Cm <sup>-1</sup>	820	820	820	820	Si-O-Si symmetric stretching vibration mode
1070 Cm <sup>-1</sup>	1070	1070	1070	1070	Si-O-Si asymmetric stretching vibration mode
-----	1311	1324	1321	1316	$\alpha$ -Fe <sub>2</sub> O <sub>3</sub>

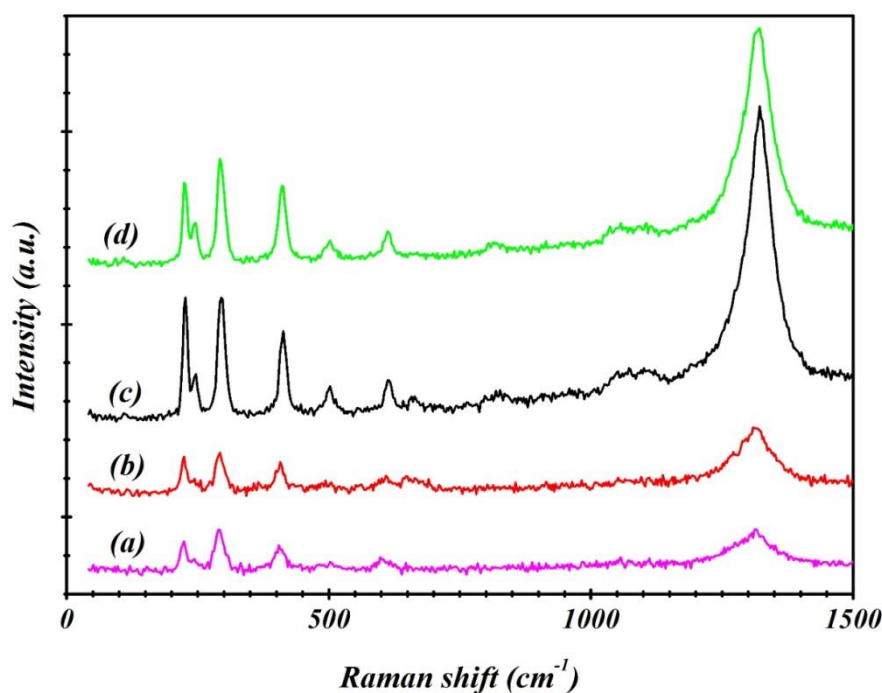


**Figure 5. Raman spectroscopy spectra of silica gel doped with different concentration of  $\alpha$ -Fe<sub>2</sub>O<sub>3</sub> (a) 3.5, (b) 11, (c) 33 and (d) 37 mol%, respectively sintered at 1170 °C**

#### **Magnetic measurements:**

The magnetic properties of  $\alpha$ -Fe<sub>2</sub>O<sub>3</sub> / SiO<sub>2</sub> nanoparticles using different concentration (3.5, 11, 33 and 37 mol%) of Fe<sub>2</sub>O<sub>3</sub> sintered at 1170 °C were drawn in Figure (6). The saturation magnetization ( $M_s$ ), remnant magnetization ( $M_r$ ) and the value of coactivity ( $H_c$ ) are presented in Table (3). The values of the saturation magnetization ( $M_s$ ) decreases from 0.813 emu/g to 0.0397 emu/g with increasing  $\alpha$ -Fe<sub>2</sub>O<sub>3</sub> from 3.5 to 33 mol%, respectively. This decreasing behavior in magnetization value is related to the changes of the crystallite size, magnetic iron oxide particles and concentration. [32] The results shows that the ( $M_s$ ) increases up to 0.0659 emu/g for  $\alpha$ -Fe<sub>2</sub>O<sub>3</sub> (37 mol%)/SiO<sub>2</sub>. This is attributed to the larger particle size of Fe<sub>2</sub>O<sub>3</sub> embedded in silica matrix. The high ( $H_c$ ) of the sample obtained at (37 mol%) of  $\alpha$ -Fe<sub>2</sub>O<sub>3</sub> may be attributed to the magneto static dipole interactions and / or the shape anisotropy in the high crystalline complex nanostructures in this work [33]. When  $\alpha$ -Fe<sub>2</sub>O<sub>3</sub> nanoparticles embedded in silica, the Si-O-Fe bond has been formed. The magnetic moment of iron ions of  $\alpha$ -Fe<sub>2</sub>O<sub>3</sub> nanoparticles disappeared through the Si-O-Fe connection and as a result, the magnetization decreased.

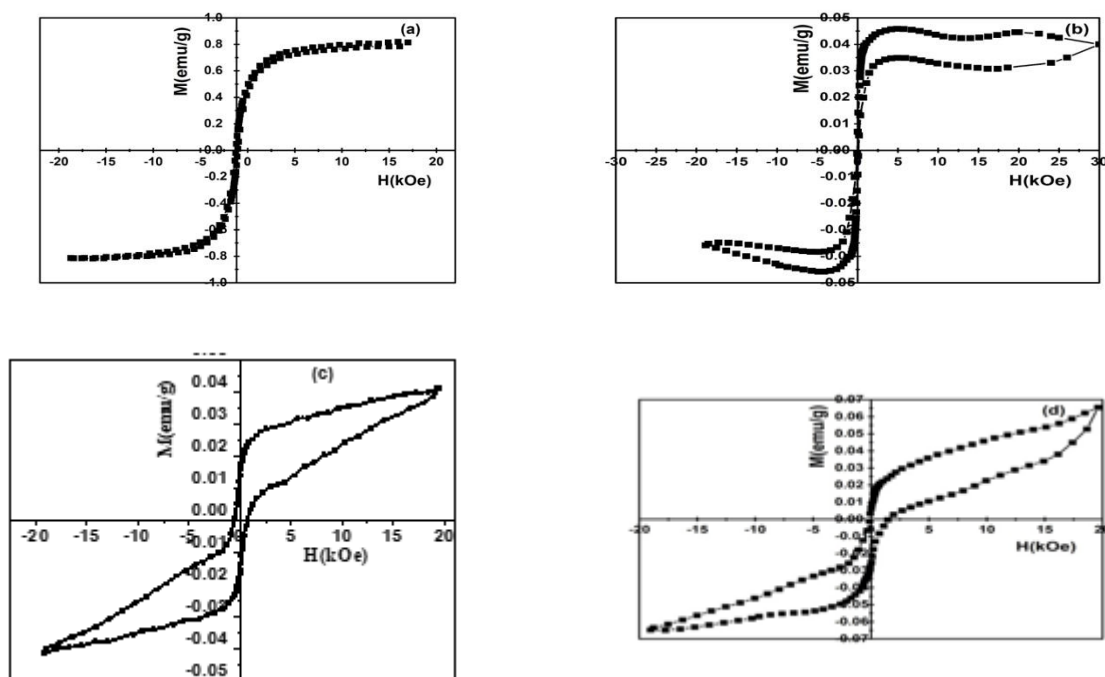


Figure 6. Magnetic hysteresis curves of silica gel doped with different concentration of  $\alpha$ -Fe<sub>2</sub>O<sub>3</sub> (a) 3.5,(b) 11, (c) 33and(d) 37mol%, sintered at 1170 °C

Table (3) The ( $H_C$ ), ( $M_R$ ), ( $M_S$ ) and ( $M_R/M_S$ ) of silica gel doped with different concentration of  $\alpha$ -Fe<sub>2</sub>O<sub>3</sub> (a) 3.5,(b) 11, (c) 33and(d) 37mol%, sintered at 1170 °C

Sample	( $H_C$ ) (kOe)	$M_R$ emu/g	$M_S$ emu/g	$M_R/M_S$
3.5	0.0387	0.2325	0.8138	0.2856
11	0.4641	0.03056	0.0458	0.6672
33	0.5477	0.02125	0.0397	0.5343
37	1.367	0.01593	0.0659	0.2417

---

**Dielectric and Conductivity properties:**

The AC conductivity  $\sigma_{ac}$  of  $\alpha$ -Fe<sub>2</sub>O<sub>3</sub> / SiO<sub>2</sub> nanoparticles using different concentration (3.5, 11, 33 and 37 mol%) of Fe<sub>2</sub>O<sub>3</sub> sintered at 1170°C in frequency range (1MHz-1GHz) illustrated in figure(7). The figure shows that  $\sigma_{ac}$  increases by increasing frequency. The observed conductivity in the lower frequency can be attributed to the weakly localized carriers which drift over large distances. At higher frequency the mean displacement of these carriers is reduced to show proximity in the conductivity [34]. Also it can be noticed that,  $\sigma_{ac}$  increased by increasing the Fe<sub>2</sub>O<sub>3</sub> content, this may be due to the increasing in the mobility of the free charge carriers in silica matrix [35]. The lower values of  $\sigma_{ac}$  for Fe<sub>2</sub>O<sub>3</sub>(3.5 mol%)/SiO<sub>2</sub> should be assigned to its particles size (25 nm), which leads to a decrease of the free ions number [36]. However, the higher values of  $\sigma_{ac}$  at higher iron oxide concentration (37 mol%) with particle size (31 nm)[37]. Hence, it may be understood here that the particle size plays an important role in conductivity [38].

The dielectric constant ( $\epsilon'$ ) and Dielectric loss ( $\epsilon''$ ) of  $\alpha$ -Fe<sub>2</sub>O<sub>3</sub>/SiO<sub>2</sub> nano particles sintered at 1170°C were also studied in the frequency range (1MHz-1GHz) in figures (8, 9). It was observed that the ( $\epsilon'$ ) and ( $\epsilon''$ ) showed the same decreasing trend with increasing frequency. This observed decrease might be according to the charge carriers scattering and the electric field fast variation accompanied with the frequency, which leading to random orientation of the dipole moments. It can be noticed that, ( $\epsilon'$ ) and ( $\epsilon''$ ) detect an increasing behavior by increasing  $\alpha$ -Fe<sub>2</sub>O<sub>3</sub> content. This increase in dielectric constant may be attributed to the decrease of the distance between grains [39]. The dielectric properties of ferrites are dependent upon several factors: including the method of preparation, chemical composition, grain structure and particle size [40]. So the observed dielectric increasing behavior of our samples may be due to the increase in the particle size (25-31) nm of Fe<sub>2</sub>O<sub>3</sub> concentration (3.5-37mol%).

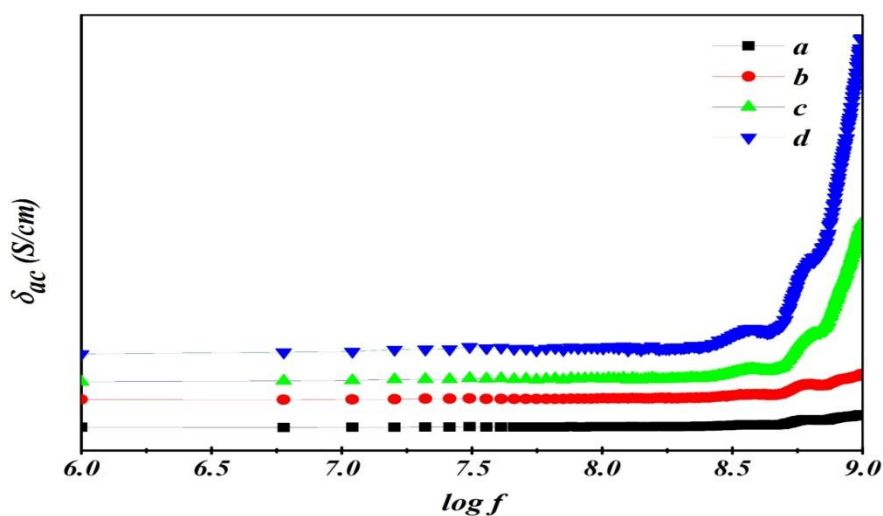


**Fig.7:** The  $\sigma_{ac}$  variation against frequency of silica gel doped with different concentration of  $\alpha\text{-Fe}_2\text{O}_3$  (a) 3.5,(b) 11, (c) 33and(d) 37mol%, sintered at  $1170^\circ\text{C}$  in frequency range ( $10^6\text{-}10^8$ ) Hz.

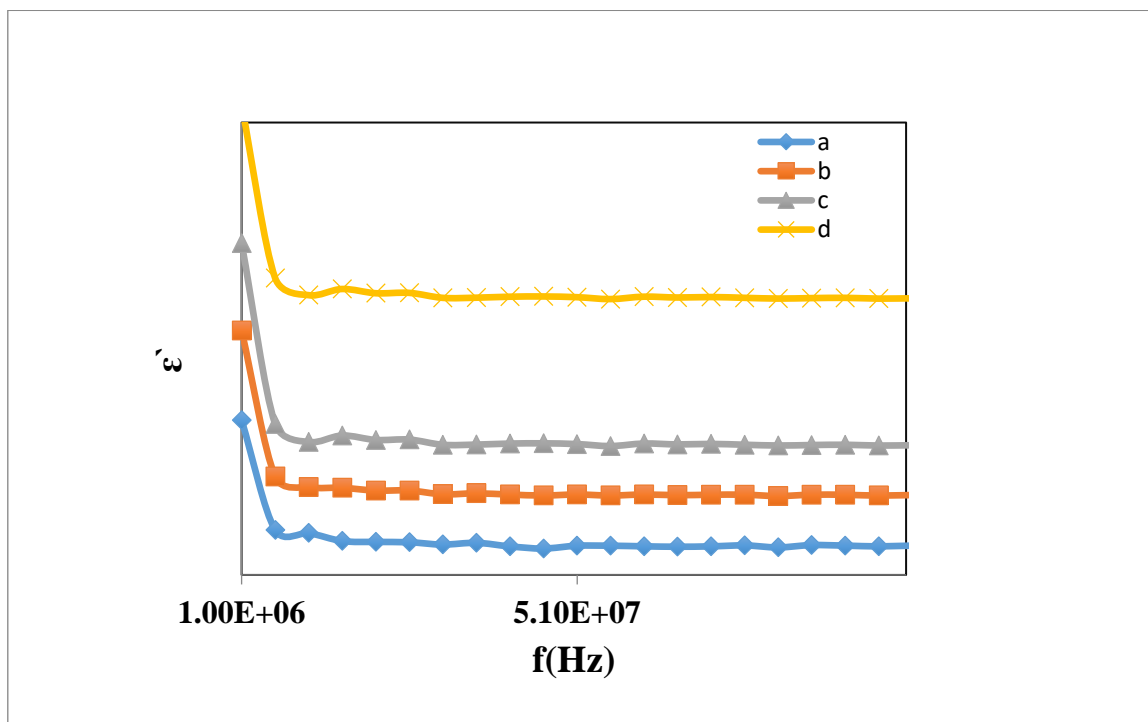


**Fig. 8:** The  $\epsilon''(\omega)$  variation against frequency of silica gel doped with different concentration of  $\alpha\text{-Fe}_2\text{O}_3$  (a) 3.5,(b) 11, (c) 33and(d) 37mol%, sintered at  $1170^\circ\text{C}$  in frequency range ( $10^6\text{-}10^8$ ) Hz.

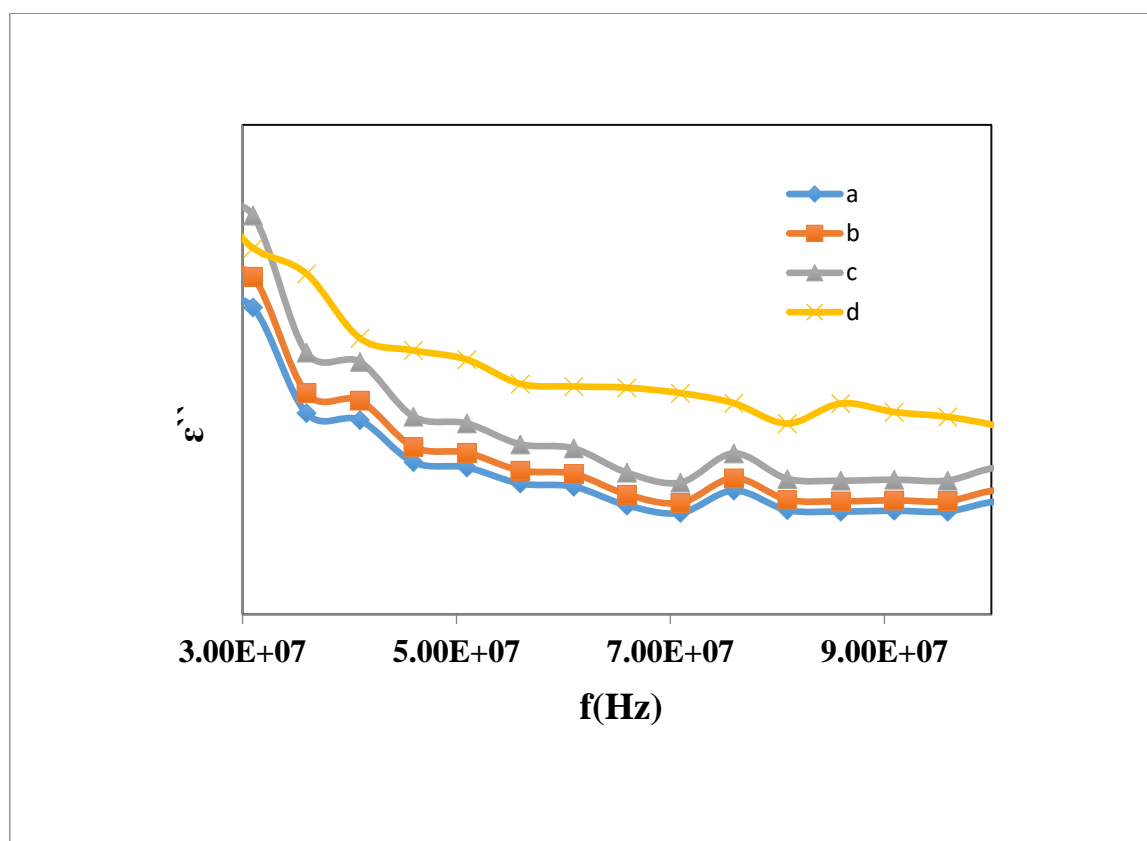


**Figure 9.** The  $\epsilon''(\omega)$  variation against frequency of silica gel doped with different concentration of  $\alpha\text{-Fe}_2\text{O}_3$  (a) 3.5, (b) 11, (c) 33 and (d) 37 mol%, sintered at  $1170^\circ\text{C}$  in frequency range ( $10^6\text{-}10^8$ ) Hz.

## Conclusion

In the present work, the silica-gel glasses doped with different concentrations of  $\text{Fe}_2\text{O}_3$ , and their structural, dielectric, magnetic and morphological trends have been evaluated. The Silica-gel doped with different concentrations of  $\text{Fe}_2\text{O}_3$  (3.5, 11, 33 and 37 mol. %) were prepared by sol gel process. The used process give rise to hematite  $\alpha\text{-Fe}_2\text{O}_3/\text{SiO}_2$  phase annealed at  $1170^\circ\text{C}$  with homogenous distribution of the nanoparticles. In addition the X-ray measurements detect the hematite phase presence. Moreover, the iron oxide embedded in silica gel host material is always in nano-structure range. The SEM measurements confirm the nano-scale presence; it is enhanced by high  $\alpha\text{-Fe}_2\text{O}_3$  concentration in the mentioned prepared samples. The Laser Raman is used to clarify the structural group's presence. The dielectric properties will be studied in frequency range (1MHz-1GHz) for first time. The obtained data revealed that the A.C. conductivity  $\sigma_{ac}$  increased by increasing the  $\text{Fe}_2\text{O}_3$  content at (3.5, 11, 33 and 37% mol. %), the dielectric permittivity increases. Finally, the values of the saturation

magnetization ( $M_s$ ) decreases from 0.813 emu/g to 0.0397 emu/g with increasing  $\alpha$ -Fe<sub>2</sub>O<sub>3</sub> from 3.5 to 33mol%, respectively. This decreasing behavior in magnetization value is related to the changes of the crystallite size, magnetic iron oxide particles and concentration. The all results supplied a new strategy to design and prepared the high – temperature photonic crystals, thermal protects and magnetic materials.

**Consent for publication:** All authors are accepting the manuscript for publication.

**Availability of data and material:** All data and material are available if required.

**Competing interests:** The authors declare no conflicts of interest regarding the publication of this paper.

**Funding:** None.

**Authors' contributions:**

- **R.K. Abd El-Hamid**, Sharing in the data analysis, drawing the figures, sharing in the manuscript drafting, preparing it for the publication, and manuscript submission.
- **N.A.M. Shahin**, Sharing in the data analysis, drawing the figures, sharing in the manuscript drafting, preparing it for the publication.

**Acknowledgements**

The Authors acknowledge Prof. Dr. I.K. Battisha; Sol gel Lab, Solid State Physics Department, Physics Research Institute and Electric and dielectric measurements unit, National Research Centre, (NRC), Physics Research Institute, Dokki, Giza 12622, Egypt. (Affiliation ID: 60014618). For her help in this work.

**Reference:**

- [1] Fawzy A. Mahmoud, Hagar Mohamed , M.B.S. Osman, “Structural and electrical properties of Sprayed ZnO:Al thin films”, Journal of Scientific Research in Science ,39-46,(2015)
- [2] Jyoti Yadav, Rimpay Shukla , "Microstructural and optical properties of Ni-doped Fe<sub>2</sub>O<sub>3</sub> nanoparticles prepared via Sol Gel Method", International journal of creative research thoughts (IJCRT), volume 10, issue 1 January (2022), ISSN:2320-2882
- [3] P. Mallick, B.N. Dash, "X-ray Diffraction and UV-Visible Characterizations of  $\alpha$ -Fe<sub>2</sub>O<sub>3</sub> Nanoparticles Annealed at Different Temperature", Nanosci.Nanotechnol.3(2013)130–134. doi:10.5923/j.nn.20130305.04.
- [4] Eman. K Tawfik, Wael H.Eisa, N. Okasha, H.A.ashry. “Influence of annealing temperature of  $\alpha$ - Fe<sub>2</sub>O<sub>3</sub> nanoparticles on Structure and Optical Properties”. Journal of Scientific Research in Science, Vol. (37), 2020
- [5] T. Ohmori, H. Takahashi, H. Mametsuka, E. Suzuki, "Photocatalytic oxygen evolution on a -Fe O films using Fe<sup>3+</sup> ion as a sacrificial oxidizing agent, (2000) 3519–3522. <https://doi.org/10.1039/B003977M>
- [6] X. Gou, G. Wang, J. Park, H. Liu, J. Yang, "Monodisperse hematite porous nanospheres: Synthesis, characterization, and applications for gas sensors", Nanotechnology.19(2008).doi:10.1088/0957-484/19/12/125606.
- [7] H. Zhou, S.S. Wong, A Facile and Mild Synthesis of 1-D ZnO , 2 (n.d.).
- [8] R. Lawaczeck, M. Menzel, H. Pietsch, Superparamagnetic iron oxide particles: Contrast media for magnetic resonance imaging, Appl. Organomet. Chem. 18 (2004) 506–513. doi:10.1002/aoc.753.
- [9] D. Walter, Characterization of synthetic hydrous hematite pigments, Thermochim. Acta .199–195 (2006) 445. doi:10.1016/j.tca.2005.08.011.

- [10] M. Busch, M. Gruyters, H. Winter, "Spin polarization and structure of thin iron oxide layers prepared by oxidation of Fe (110)", *Surf.Sci*–4166(2006)600.4169doi:10.1016/j.susc.2006.01.140.
- [11] Deepika P Joshi, Geeta Pant, Neha Arora, Seema Nainwal "Effect of solvents on morphology, magnetic and dielectric properties of ( $\alpha$ -Fe<sub>2</sub>O<sub>3</sub>@SiO<sub>2</sub>) core-shell nanoparticles", *Heliyon* 3 (2017) <https://doi.org/10.1016/j.heliyon.2017.e00253>
- [12] H.H. MAHMOUD, I. K.BATISHA AND F. M. EZZ-ELDIN, STRUCTURAL, OPTICAL AND MAGNETIC PROPERTIES OF  $\Gamma$ -IRRADIATED SiO<sub>2</sub> XEROGEL DOPED Fe<sub>2</sub>O<sub>3</sub>, *J. SPECTROCHIMICA ACTA PART A: MOLECULAR AND BIOMOLECULAR SPECTROSCOPY*, 150, 72-82, (2015). [HTTPS://DOI.ORG/10.1016/J.SAA.2015.05.011](https://doi.org/10.1016/j.saa.2015.05.011)
- [13] MACHALA L, ZBORIL R, GEDANK A, CORRECTION TO POLYMORPHOUS TRANSFORMATIONS OF NANOMETRIC IRON (III) OXIDE: A REVIEW (2007) *J PHYS CHEM B* 111:4003–4018. DOI: 10.1021/cm2021824
- [14] Sanaa S. Zaki, Kheiralla Z. H., Rushdy A. A, Betiha M.A. and Hanan B. Abousittash, "Embedded Mesoporous Silica Silver Nanoparticles as potential antibacterial agent against Multidrug-Resistant Bacteria", *Journal of Scientific Research in Science* , 158-178,(2017)
- [15] NAKAMURA T, YAMADA Y, YANO K, "NOVEL SYNTHESIS OF HIGHLY MONODISPersed  $\Gamma$ -Fe<sub>2</sub>O<sub>3</sub>/SiO<sub>2</sub> AND  $\epsilon$ -Fe<sub>2</sub>O<sub>3</sub>/SiO<sub>2</sub> NANOCOMPOSITE SPHERES", (2006) *J MATER CHEM* 16:2417–2419. [HTTPS://DOI.ORG/10.1039/B604025J](https://doi.org/10.1039/B604025J)
- [16] S.A.Salehizadeh, M.P.F.Graca, and M.A.Valente, Effect of ion on the dielectric properties of silicate glasses prepared by sol-gel *Phys. Status Solidi*, 11,9(2014)1455-1458. <https://doi.org/10.1002/pssc.201400015>
- [17] Rajesh v. Pai , Rasmi Morajkar, Nitin Gumber, A.M.Banerjee, and Sher Singh Meena, "Preparation of silica Xerogel beads embedded with Fe<sub>2</sub>O<sub>3</sub> nanoparticules and their characterization " *Journal of Nanopartical Research* 23 (10), 1-18 (2021). <https://doi.org/10.1007/s11051-021-05330-1>
- [18] Ashish Nadar, Atindra Mohan Banerjee, M.R.Pai, Sher Singh Meena, R.V. Pai, R.Tewari, S.M.Yusuf, A.K. Taripathi, and S.R.Bharadwaj, "Nanostructure Fe<sub>2</sub>O<sub>3</sub> dispersed on SiO<sub>2</sub> as catalyst for high temperature sulfuric acid decomposition – structural and morphological modifications on catalytic use and relevance of Fe<sub>2</sub>O<sub>3</sub>- SiO<sub>2</sub> interactions" *Applied Catalysis B: Environmental* 217, 154-168 (2017). <https://doi.org/10.1016/j.apcatb.2017.05.045>
- [19] I.K.Battisha, A.El Beyally and S.L.Seliman, "Structural and optical studies of nanostructure silica gel doped with different rare earth elements, prepared by two different sol-gel techniques", 8<sup>th</sup> Arab International Conference on Polymer Science and Technology, 27-30 November (2005), Cairo-Sharm El-Shiekh, Egypt
- [20] G. Ennas, A.Musinu and et al, "Characterization of Iron Oxide Nanoparticles in an Fe<sub>2</sub>O<sub>3</sub>-SiO<sub>2</sub> Composite prepared by a sol- gel method", *Chem.Mater.* 10,495-502,(1998). <https://doi.org/10.1021/cm970400u>
- [21] Ashish Nadar, Atindra Mohan Banerjee and et al, "Immobilization of crystalline Fe<sub>2</sub>O<sub>3</sub> nanoparticles over SiO<sub>2</sub> for creating an active and stable catalyst: A demand for high temperature sulfuric acid decomposition", *Applied Catalysis B: Environmental* 283(2021)119610. <https://doi.org/10.1016/j.apcatb.2020.119610>
- [22] Zhi Yang, Mingsheng Luo, Qinglong Liu, Buchang Shi, "In situ XRD and Raman Investigation of the Activation Process over K–Cu–Fe/SiO<sub>2</sub> Catalyst for Fischer–Tropsch

- Synthesis Reaction”, Catalysis Letters (2020) 150:2437–2445. <https://doi.org/10.1007/s10562-020-03147-6>
- [23] A.H.Lu, J.J.Nitz, M.Comotti and et al, “Spatially and size selective synthesis of Fe-based nanoparticles on ordered mesoporous supports as highly active and stable catalysts for ammonia decomposition”. *J.Am.Chem.Soc.* 132(2010)14152-14162. <https://doi.org/10.1021/ja105308e>
- [24] Marin Tadic\*, Matjaz Panjan, Biljana Vucetic Tadic ,Jelena Lazovic , Vesna Damnjanovic, Martin Kopani, Lazar Kopanja, “Magnetic properties of hematite ( $\alpha - \text{Fe}_2\text{O}_3$ ) nanoparticles synthesized by sol-gel synthesis method: The influence of particle size and particle size distribution”, *Journal of electrical Engineering*, VOL 70 (2019), NO-7S, 71–76. DOI: 10.2478/jee-2019-0044
- [25] Y. Lin, P.R. Abel, A. Heller, C.B. Mullins, “ $\alpha - \text{Fe}_2\text{O}_3$  Nanorods as Anode Material for Lithium Ion Batteries”, (2011) 2885–2891. <https://doi.org/10.1021/jz201363j>
- [26] S. Shaker, S. Zafarian, C.H. Chakra, K.V. Rao, “Preparation and Characterization of Magnetite Nanoparticles by Sol-gel Method for Water Treatment”, *International Journal of Innovative Research in Science Engineering and Technology* 2 (7) (2013) 2969–2973. ISSN: 2319-8753
- [27] S. A. Salehizadeh, M. P. F. Graça, and M. A. Valente, *Phys. Status Solidi C* , “Structural and impedance spectroscopy characteristics of  $\text{BaCO}_3/\text{BaSnO}_3/\text{SnO}_2$  nanocomposite: observation of a non-monotonic relaxation behavior”, 11, No. 9, 1455–1458 (2014) <https://doi.org/10.1039/C7RA12442B>
- [28] Xin Zhang, Yongan Niu, Yang Li, Yao Li, Jiupeng Zhao , “Preparation and thermal stability of the spindle  $\alpha - \text{Fe}_2\text{O}_3 @ \text{SiO}_2$  core–shell nanoparticles”, *Journal of Solid State Chemistry* 211 (2014) 69–74. <https://doi.org/10.1016/j.jssc.2013.12.011>
- [29] Kim, C. S., Shin, J. W., An, S. H., Jang, H. D., & Kim, T. O. “Photodegradation of volatile organic compounds using zirconium-doped  $\text{TiO}_2/\text{SiO}_2$  visible light photocatalysts”. *Chemical engineering journal*, 204, (2012),40-47. <https://doi.org/10.1016/j.cej.2012.07.093>
- [30]- H. Zhang, A. Xie, C. Wang, H. Wang, Y. Shen, X. Tian, “Novel rGO/ $\alpha - \text{Fe}_2\text{O}_3$  composite hydrogel: Synthesis, characterization and high performance of electromagnetic wave absorption”, *J. Mater. Chem. A*. 1 (2013) 8547–8552. doi:10.1039/c3ta11278k.
- [31] Fu D, Dai W, Xu X, Mao W, Su J, Zhang Z, Shi B, Smith J, Li P, Xu J, Han Y-F “Probing the structure evolution of iron-based Fischer–Tropsch to produce olefins by operando Raman spectroscopy”. *Chem.Cat.Chem* 7(5):752–756, (2015) <https://doi.org/10.1002/cctc.201402980>
- [32] Ahmad Taufiq, Ainun Nikmah, Arif Hidayat, Sunaryono Sunaryono, Nandang Mufti, Nurul Hidayat, Hend raSusanto b, 16 UM Lecturers Are Included in the 500 Best Indonesian Researchers in SINTA Version Elsevier (2020)
- [33] O. Karaagac, H. Kockar, “A simple way to obtain high saturation magnetization for superpara-magnetic iron oxide nanoparticles synthesized in air atmosphere: Optimization by experimental design”, *J. Magn. Mater.* 409 (2016) 116–123. <https://doi.org/10.1016/j.jmmm.2016.02.076>
- [34] S. Das and S. Chaudhuri, “Temperature dependent dielectric relaxation and electrical conductivity in single layer  $\text{ZnO}-\text{Al}_2\text{O}_3$  nanocomposite thin films”, *phys. stat. sol. (b)*, 244(2007) 2657–2665. <https://doi.org/10.1002/pssb.200642287>

- 
- [35] H. M.GOBARA AND M. M.GOMAA, "ELECTRICAL PROPERTIES OF NI/SILICA GEL AND PT/ $\gamma$ -ALUMINA CATALYSTS IN RELATION TO METAL CONTENT IN THE FREQUENCY DOMAIN", MATERIAL CHEMISTRY AND PHYSICS 113(2009)790-796. [HTTPS://DOI.ORG/10.1016/J.MATCHEMPHYS.2008.08.058](https://doi.org/10.1016/j.matchemphys.2008.08.058)
- [36] Mahmoud Mohammed Ismail, Hazem FAROUK AHMED, Lidia Zur, Alessandro Chiasera, Maurizio Ferrari, Anna Lukowiak, Adel Ashery, Mohamed Ali, Inas Kamal Battisha, "Optical, structure and dielectric properties of Er<sup>+3</sup> ions doped Al-Na-K-Ba phosphate glasses", Egyptian Journal of Chemistry, Egypt. J. Chem. 63, (10), (2020)(1-14). <https://doi.org/10.21608/ejchem.2020.27059.2578>
- [37] K.P. Padmasree, D.K. Kanchan, A.R. Kulkarni," Impedance and Modulus studies of the solid electrolyte system 20CdI<sub>2</sub>-80[xAg<sub>2</sub>O-y(0.7V<sub>2</sub>O<sub>5</sub>-0.3B<sub>2</sub>O<sub>3</sub>)], where 1 ≤x/y ≤ 3",Solid State Ion.177, 475-482 (2006). <https://doi.org/10.1016/j.ssi.2005.12.019>
- [38]S. M. Reda, "Electric and dielectric properties of Fe<sub>2</sub>O<sub>3</sub>/Silica Nanocomposites", International Journal of Nano Science and Technology Vol. 1, No. 5, June (2013), PP: 17 - 28, ISSN: 2328-5443
- [39] H.Darwish, M.M.Gomaa, "Effect of compositional changes on the structure and properties of alkali-alumino borosilicate glass".J.Mater.Sci. Mater. Electron, 17(1)(2006)35-42.
- [40] V. A. Hiremath and A. venkataraman, "Dielectric, electrical and infrared studies of  $\gamma$ -Fe<sub>2</sub>O<sub>3</sub> prepared by combustion method", Bull. Mater. Sci. 26 (2003) 391-396.

## المخلص العربى

التحليل الطيفى الدقيق بالليزر Raman وخصائص العزل الكهربائى عالية التردد للسيليكا-xerogel  
محملة بتركيزات مختلفة من  $\alpha\text{-Fe}_2\text{O}_3$ 

اريهام كمال عبد الحميد – انجلاء احمد شاهين

<sup>1</sup>كلية النبات للاداب والعلوم والتربيه , جامعة عين شمس, قسم الفيزياء

فى هذا البحث تم تحضير مركبات  $\text{Fe}_2\text{O}_3/\text{SiO}_2$  السليكا جل النانومتريه والمطعمه بتركيزات مختلفة من اكسيد الحديد ( 37 mol % and 11,33,5. ) وتسخينها عند درجة حراره (  $1170^\circ\text{C}$  ). اظهرت نتائج حيود الاشعه السينيه وجود بلورات سيليكا رباعيه  $\alpha$ -cristobalite كما اظهرت وجود مراحل الحديد المختلفة وهى Hematite( $\alpha\text{-Fe}_2\text{O}_3$ ) مع قليل من  $\gamma\text{-Fe}_2\text{O}_3$  (Magnetite),  $\epsilon\text{-Fe}_2\text{O}_3$  (Maghemite). وبزيادة تركيز الحديد ظهرت قمم ضيقه وحاده دليل على زيادة بللوريه العينه بزيادة نسبة الحديد. عند درجات الحراره المنخفضه تكون مراحل الحديد الموجوده هى (  $\gamma\text{-Fe}_2\text{O}_3$  او  $\epsilon\text{-Fe}_2\text{O}_3$  ) وهذا يرجع الى بطء اكسدة ايونات الحديد اما زيادة درجة الحراره الى  $1170^\circ\text{C}$  يؤدى الى سرعه اكسدة ايونات الحديد مما يسبب تحول مراحل الحديد من Maghemite الى Hematite . وبحساب الحجم الجزيئى للمركبات وجد انها تزيد من 25 الى 31 نانومتر بزيادة نسبة الحديد. وباستخدام الميكروسكوب الالكترونى النافذ (TEM) وجد ان متوسط الحجم الجزيئى للعينات 24 نانومتر مما يتفق مع نتائج XRD . بينما صور الميكروسكوب الالكترونى الماسح (SEM) اوضحت تجانس توزيع الجزيئات دون اى تكتلات ولها شكل بللورى رباعى الزوايا -  $\alpha$  cristobalite . من خلال قياسات Raman للعينات المحضره اوضحت وجود  $\alpha$ -cristobalite و ( $\alpha\text{-Fe}_2\text{O}_3$ ) مما يتفق مع نتائج XRD . وبدراسة الخصائص الكهربيه للمركبات فى مدى تردد ( 1 MHz - 1 GHz ) وجد ان التوصيليه الكهربيه  $\sigma_{AC}$  تزيد بزيادة التردد وهذا يرجع الى وجود حاملات الشحنة التى تتحرك فى اتجاه المجال الكهربى مما يتسبب فى تدفق الشحنات عبر العينه. اما بزيادة تركيز الحديد فذلك يؤدى الى زيادة حركة حاملات الشحنة داخل سلسله السيليكا مما يؤدى الى زيادة التوصيليه الكهربيه  $\sigma_{AC}$ . وبقياس خصائص العزل عند الترددات المنخفضه يكون قيم  $\epsilon'$  و  $\epsilon''$  كبيره وبزيادة التردد تقل قيمتهما وذلك لعدم قدرة حاملات الشحنة على تتبع الزيادة فى المجال الكهربى. كما وجد ان قيم  $\epsilon'$  و  $\epsilon''$  تزيد بزيادة تركيز اكسيد الحديد. وبدراسة تأثير زيادة نسبة الحديد على الخصائص المغناطيسيه للعينات يتضح ان المغناطيسيه تقل بزيادة نسبة الحديد. ومن نتائج القياسات وجد ان ال Hematite هو اكثر انواع الحديد استقرارا فى الظروف المحيطه وكذلك تحت تأثير درجات الحراره العاليه لذلك يفضل استخدامه فى معظم التطبيقات .